Cite this article as:
Scargiali F., Busciglio A., Grisafi F., Brucato A., Free surface oxygen transfer in large axpect ratio unbaffled bio-reactors, with or without draft-tube, *Biochemical Engineering Journal*, 100 (2015) 16-22.
http://dx.doi.org/10.1016/j.bej.2015.04.006

FREE SURFACE OXYGEN TRANSFER IN LARGE ASPECT RATIO UNBAFFLED BIO-REACTORS, WITH OR WITHOUT DRAFT-TUBE

Scargiali F.[a], Busciglio A.[b], Grisafi F.[a], Brucato A.[a]

[a]*Dipartimento di Ingegneria Chimica, Gestionale, Informatica e Meccanica*
Università di Palermo, Viale delle Scienze, Ed.6, 90128 Palermo (Italy)
[b]*Dipartimento di Chimica Industriale "Toso Montanari"*
Alma Mater Studiorum – Università di Bologna, via Terracini 34, 40131 Bologna, Italy

Abstract: It is widely accepted that animal cell damage in aerated bioreactors is mainly related to the bursting of bubbles at the air–liquid interface. A viable alternative to sparged bioreactors may be represented by uncovered unbaffled stirred tanks, which have been recently found to be able to provide sufficient mass transfer through the deep free surface vortex which takes place under agitation conditions. As a matter of fact, if the vortex is not allowed to reach impeller blades, no bubble formation and subsequent bursting at the free-surface, along with relevant cells damage, occurs.

In this work oxygen transfer performance of large aspect ratio unbaffled stirred bioreactors, either equipped or not with an internal draft tube, is presented, in view of their use as a biochemical reactors especially suited for shear sensitive cell cultivation.

Keywords: Bioreactors; Mixing; Mass Transfer; Oxygen Transfer; Free Surface.

Corresponding author:

Francesca Scargiali,

Dipartimento di Ingegneria Chimica, Gestionale, Informatica e Meccanica

Università di Palermo, Viale delle Scienze, Ed.6, 90128 Palermo (Italy)

e-mail address: francesca.scargiali@unipa.it

tel: +39 09123863714

1. INTRODUCTION

Gas–liquid stirred vessels are widely employed to carry out aerobic fermentations as well as chemical reactions involving a gas reagent and a liquid phase. For low viscosity liquids, the cylindrical vessel walls are typically equipped with swirl-breaking baffles, aimed at improving mixing performance. In fact, in the absence of swirl-breaking baffles, the relative velocities between the highly swirling liquid and stirrer blades are generally lower than those observed in baffled vessels: this results into smaller pumped flow rates and, in turn, into poorer mixing than in baffled tanks [1].

Despite allegedly being poorer mixers than baffled vessels, unbaffled stirred tanks are recently enjoying a growing interest in the process industry, as they provide significant advantages in a number of applications where the presence of baffles is undesirable for some reason [2]. This is for instance the case of crystallizers, where the presence of baffles may promote encrustations [3], or in food and pharmaceutical industries, where vessel cleanness is a topic of primary importance [4]. In bioslurry reactors for soil remediation processes, sufficient oxygen transfer may be guaranteed by the central vortex formation as an alternative to the adoption of gas spargers, which are intrinsically more troublesome [5]. As a matter of fact, solid particles could cause wear of the sparger holes, or the particles may form a muddy solid residue that blocks sparger holes. Such phenomena have adverse effects on the performance of the sparger and favour the adoption of unbaffled reactors or gas inducing impellers. When dealing with robust cells and non-foaming systems, liquid aeration can be further increased by adopting rotational speeds large enough to promote gas ingestion from the suface or by using a self-ingesting device [6-8]

Notably, when a suspended solid phase is present, higher values of the solid-liquid mass transfer coefficients may be obtained in unbaffled vessels, at the same value of mechanical power

dissipation [9]. Also the mechanical power required to achieve complete suspension is found to be smaller than in baffled vessels [5, 10].

As regards shear sensitive cell cultivations, mechanical agitation and especially bubble bursting at the free surface, unavoidably associated to air sparging, can cause cell death [11, 12]. In unbaffled vessels a free surface deep vortex takes place under agitation conditions [13]. At agitation speeds such that the free-vortex bottom does not reach the impeller plane (*subcritical conditions*) , no bubbles are dispersed in the liquid phase and therefore the cell damage associated with bubble bursting is avoided altogether. Under such conditions, the oxygen mass transfer that takes place through the vortex surface was shown to be sufficient for typical animal cell cultures [14]. This feature clearly makes unbaffled vessels potentially advantageous for shear sensitive cultures (e.g. animal cell or filamentous mycelia cultures), as well as for many foaming gas-liquid systems that share the need to avoid bubble dispersion in the liquid phase, provided that process rates, and relevant gas consumption needs, are compatible with the relatively small gas transfer rates achievable [14]. In the above works fairly "standard" unbaffled vessels were investigated, especially as it regards vessel aspect ratio (always equal to one). Considering the encouraging results there obtained, one might wonder whether geometry changes such as the adoption of larger aspect ratios and/or the installation of an internal draft tube, may give rise to advantages in the realm of bioreactor applications. As a matter of fact, increasing liquid height is expected to increase the maximum agitation speed at which the agitator may be operated without gas ingestion, that should positively affect OTR, though on the other hand the liquid volume to feed is increased as well, so that this geometry change might result in either improved or worsened culture oxygenation with respect to standard aspect ratio vessels. Another geometry change that might improve culture oxygenation is the introduction of a draft tube, that should improve mixing rates while shortening vortex height, so allowing the adoption of larger agitation speeds and relevant improved OTR, still

in the absence of bursting bubbles and associated cell damage effects. On the basis of the above considerations, in this work oxygen transfer performance of large aspect-ratio unbaffled stirred reactors, either equipped or not with an internal draft tube, is investigated in view of their use as biochemical reactors for shear sensitive cell cultivation.

2. EXPERIMENTAL

The investigated reactor is depicted in Fig.1. It consisted of a flat bottomed cylindrical tank with an internal diameter of 280 mm and an height of 1450 mm (Fig. 1a). In some configurations (Fig. 1b and 1c) a removable internal cylindrical concentric draft-tube with internal diameter of 194 mm, thickness of 3 mm and length of 500 mm, off-spaced from vessel bottom by 60 mm, was mounted inside the vessel by means of suitable supports and rod spacers. A 0.095 m diameter six-flat-blade (blade height = 19 mm) hub-mounted turbine was installed on the 17 mm dia. shaft, below the draft-tube, at a clearance C=30 mm. Notably the purpose of placing the stirrer as close as possible to vessel bottom was that of maximizing water height above it and therefore maximizing the agitation speed achievable before vortex reached the impeller and air started to be dispersed in the liquid phase. For the small clearance impeller a turbine with radial action was deemed to be a better choice than an axial turbine.

Stirrer shaft was driven by a 1200W DC motor (Mavilor MSS-12), equipped with tacho and speed control unit (Infranor SMVEN 1510) so that rotational speed was maintained constant, with a maximum deviation of 0.1% from the set point. Rotational speeds ranged from 100 to 1100 rpm in order to explore different fluid-dynamic regimes occurring inside the unbaffled stirred reactor. The vessel was filled with deionized water. Depending on the experimental run, liquid eight under no agitation conditions was either 280 mm (H=T), or 560 mm (H=2T), or 840 mm (H=3T) above vessel bottom. In the cases of H=2T and H=3T both the configurations with and without draft tube were investigated. It is worth noting that in the case H=2T the liquid level at rest coincides with the draft tube brim. This was chosen to see whether, while in operation, the more complex flow field in the vicinities of the brim could result in improved mass transfer performance.

Power consumption was measured by monitoring the temperature rise due to agitation power input [7, 8]. All temperature dynamics showed a remarkably constant slope. For simplicity, in the computation of power dissipation the heat capacity of vessel walls, shaft and impellers were neglected in front of that of the water mass. Also, heat exchange through vessel walls was neglected, on the basis of the very small temperature differences between water and ambient air (smaller than 0,5 °C, as each run was started from equilibrium conditions with the surroundings). This allowed to directly convert the observed temperature rise speed (e.g. 3.07 10^{-4} °C/s at 850 rpm) into the relevant specific dissipation rate (1.56 W/kg). It can be stated that power consumption so computed is slightly smaller than the actual value, because of the already mentioned simplifications; however the resulting underestimation was considered to be negligible for engineering purposes. The total agitation power was finally estimated by multiplying specific power dissipation by the system water mass (e.g. 34.5 kg, H=2T).

The volumetric mass transfer coefficient, k_La, was assessed *via* unsteady-state experiments by means of the simplified dynamic pressure method (SDPM) [15], a technique that was found to be particularly suitable for k_La assessment in culture media and fermentation broths [14]. In this method the driving force for oxygen absorption is obtained by a sudden change of vessel pressure, with no need for sudden gas phase composition changes. For a perfectly mixed system, if k_La and the interfacial gas concentrations are identical for all bubbles at any time, equation (1) is obtained:

$$k_L a = -\frac{1}{t - t_0} \ln\left(\frac{C_L^* - C_L}{C_L^* - C_L^0}\right) \qquad (1)$$

where C_L^0, C_L and C_L^* are the initial (time zero), instantaneous (at time t) and interfacial (*viz* equilibrium) oxygen concentration in the liquid phase, respectively. Eqn.1 shows that, if the above

hypothesis are reasonably satisfied, plots of $ln(C_L^* - C_L)$ versus t should result into straight lines with a slope equal to ($-k_La$). This is not rigorously true, due to the contemporaneous nitrogen transport effects, but these can be accounted for by applying a correction factor to the measured slopes, as described in Scargiali and co-workers [15]. This correction however becomes significant only for quite large k_La values, and in practice was never needed in the present work.

An inexpensive Venturi vacuum pump (Vaccon HVP 100), fed by compressed air, was used to evacuate the vessel down to an inside initial pressure of about 0.1 bar. An electrode sensor (WTW CellOx 325) and control unit (WTW Oxi 340i) were used in order to measure oxygen concentration in the liquid phase. The probe time constant was of the order of 3 seconds, and never interfered with k_La measurements (the relevant discussion may be found in Scargiali *et al*. [15]). The output of the oxygen measurement unit was recorded by a data acquisition system and processed to yield the relevant value of the mass transfer coefficient k_La.

In all runs temperature inside the reactor was between 20 and 21 ^oC. This was obtained by adjusting the initial temperature to a value equal to the room temperature ±0.5°C, and exploiting the circumstance that the temperature increase during each single run was always less than 0.2 ^oC.

3. RESULTS AND DISCUSSION

3.1 Fluid dynamic regimes

As already observed in smaller scale "standard" (aspect ratio =1.0) unbaffled stirred vessels, when the stirrer is operated at rotational speeds sufficiently small in order for vortex bottom to remain above the stirrer blades, no air is ingested in the liquid phase (*sub-critical regime*). The free-surface shapes observed in the systems without draft-tube are quite similar to each other at any agitation speed, though vertically displaced because of the different liquid volume fillings (Fig.1a). This finding could be expected, as vortex shape mainly depends on tangential velocity profile, which in

turn is known to only weakly depend on initial liquid filling [13, 16]. For the system with draft tube and H = 3T, vortex shape was found to be somewhat shallower in comparison to that observed in the absence of draft tube, clearly due to the increased fluid friction, and in turn slightly decreased average tangential velocities.

At the highest velocities vortex bottom overcomes the impeller leading to bubble injection in the liquid phase, that are then radially entrained by the impeller stream towards vessel wall. Afterwards, while moving upwards under the effect of gravity, they undergo a centripetal acceleration towards the central vortex, due to their smaller density with respect to the liquid phase. These events result in practice in the formation of a gas-liquid dispersion (*super-critical regime*) in a significant portion of vessel volume.

Notably, at the impeller speed at which vortex bottom just reaches the impeller plane no bubbles are still ingested in the liquid phase: this implies that in order to reach the *super-critical* regime, characterized by significant gas ingestion, agitation speed needs to be further increased.

3.2 *Power consumption*

The specific power dissipation values obtained at the various agitation speeds are reported in Fig. 2 for the five reactor geometries investigated: three configurations without draft tube and different liquid levels (no draft H=T; H=2T and H=3T) and two configurations with the internal draft tube and two liquid levels (draft tube H=2T and H=3T).

In Fig.2 a steep increase of power dissipation with agitation speed is observed for all configurations tested, as expected. However, power dissipation appears to follow two different dependencies on the agitation speed because of the different flow regimes: in the *sub-critical* regime, the specific power dissipation follows a power law with an exponent of about 3, while beyond some critical agitation speed, a slight reduction of the power law exponent is observed. This may well depend on

the fact that an increasingly larger portion of impeller blades falls within the vortex and, being not in contact with the liquid phase, becomes unable to contribute any more to torque [2]. Also the formation of gas pockets (called *cavities*) behind stirrer blades, commonly observed in sparged baffled gas-liquid reactors (e.g. [17, 18]) may contribute to the overall effect observed.

The relevant total power dissipation was translated into power number (N_p) values, defined as

$$N_p = \frac{P}{\rho_L N^3 D^5} \tag{2}$$

where P is agitation power, ρ_L is liquid density, N is agitation speed (s^{-1}) and D is impeller diameter. Power Number results are reported in Fig. 3 for the five cases investigated. As can be observed for all investigated configurations power number versus Reynolds plots show a slightly-decreasing behaviour as long as the free surface vortex does not reach the impeller (non-aerated regime), while a neatly decreasing trend is observed in all cases after the vortex reaches the impeller and air bubbles begin to be dispersed inside the reactor. A similar behaviour, with almost equal slopes, was previously observed by Scargiali *et al.* [2] in "standard" unbaffled stirred vessels.

It is worth noting that at the same Reynolds number (same agitation speed) power number increases as liquid height H (*viz* liquid volume) increases. This is expected in view of the larger surface friction against reactor wall, and also at the same liquid height, power number increases when the internal draft tube is present, clearly due to the larger amount of surfaces opposing liquid motion, and therefore the higher fluid friction, involved in the presence of the draft tube. Several attempts were put forward to correlate in a simple way the observed N_p values to the extent of "resisting" (i.e. stationary in the vessel reference frame) surfaces. None of these was however fully successful, probably due to the fact that the stationary surfaces give rise to larger contributions to power demand the closer they are to the stirrer.

In order to unambiguously define a *critical agitation speed* (N_{crit}) that safely ensures the absence of gas ingestion for N<=N_{crit} , the agitation speed at which the N_p *vs Re* curves neatly change their slope was adopted here. Hence N_{crit} was easily assessed as the intercept between the two straight lines characterizing log-log N_p *vs Re* plots.

For comparison purposes in Tab. 1 the various N_{crit} together with relevant *critical* Reynolds numbers (Re_{crit}), specific power inputs (P/V_{crit}) and mass transfer coefficients k_La_{crit} are reported for each investigated bioreactor configuration.

It is worth noting that, given that the vortex depth (ΔH) is generally a linear function of *Fr* number [13]:

$$\Delta H \propto Fr \propto N^2 \tag{3}$$

considering that for the present system the critical ΔH value is close to the initial liquid filling H (due to the very small impeller clearance adopted), it is expected that increasing the liquid filling from T to 2T, or from 2T to 3T, an increased value of $N_{crit\_2T} = (2/1)^{0.5} * N_{crit\_T}$ and $N_{crit\_3T} = (3/2)^{0.5} * N_{crit\_2T}$ should be found respectively. This is what approximately occurs, as it can be seen in Table 1. Hence, an increase of liquid filling increases the maximum impeller speed at which the vessel can be operated without bubble dispersion. Clearly, more accurate predictions could be obtained by suitably modelling the free surface (see for example Busciglio *et al*., [13]).

When the draft tube is used, this leads to smaller tangential velocities, hence narrower and shallower vortex. In this case, an increase of N_{crit} should be expected, and is in fact confirmed by the results reported in Table 1.

A significantly different behavior is observed in the case of the system filled up to H = 2T and equipped with the draft tube (Fig. 1c). In this case, in fact, the initial liquid filling equals the upper section of the draft tube. Hence, when the agitator is started, the annulus liquid level starts to increase until it *falls* inside the central section. A very narrow vortex is formed within the draft

tube, as depicted in Fig.1c. In this case the effect on fluid velocity is maximum, and a larger effect of the draft tube presence on N_{crit} is observed than in the H = 3T cases, as it can be appreciated in Table 1.

3.3 Gas-liquid mass transfer

The k_La values obtained by means of the SDPM technique in the three configurations without draft tube are reported in Fig. 4 as a function of rotational speed. In the same figure black symbols mark critical agitation speed (N_{crit}) and relevant mass transfer coefficients (k_La_{crit}) at which the free surface vortex reaches the impeller. As it is possible to see, for all three liquid levels here investigated, the mass transfer coefficient increases as agitation speed is increased, while at the same rotational speed the specific mass transfer coefficient decreases when liquid volume is increased. This finding can be explained observing that at the same rotational speed N, when increasing liquid volume similar free surface shapes (same absolute interfacial area) and gas-liquid relative velocities are obtained, while an increasing different liquid volume is to be considered.

It is worth noting that in order to avoid gas dispersion inside the reactor, so preserving cells from bubble burst damage, an operating agitation speed smaller than the critical one (N_{crit}) is recommended. In the present system this practically implies a maximum k_La value of the order of $1.7 * 10^{-3}$ s^{-1} independently of liquid height, as highlighted in Table 1 or by the black symbols in Fig. 4. This value is much higher than the minimum value of about $2.8 * 10^{-4}$ s^{-1} required to support animal cell cultures at a typical culture concentrations of about 10^6 cells/ml [19]. Hence, it can be concluded that the investigated bioreactor, when operated at sufficiently high sub-critical agitation speeds, is fully able to satisfy the Oxygen Transfer Rate demand of current animal cell cultures, independently of the liquid aspect ratio configuration.

As concerns power requirements, in Fig. 5 the same data of Fig. 4 are reported versus *specific power input*. Results indicate that the higher the H/T the larger the specific power dissipation required to achieve the same k_La values. This implies that better energy efficiency is obtained by adopting relatively small *H/T* ratios, though larger aspect ratios are likely to be preferred for larger scale operations, because of heat transfer requirements. Notably, power demand is unlikely to be a factor of major concern in the targeted applications.

It may be worth noting that, for each data set and starting from the points at the lowest agitation speed (lowest power dissipation), the observed k_La increase is likely to be mainly due to k_L increase as long as the vortex depth is not too pronounced, while a steeper dependence of k_La on *P/V* can be observed near the critical points, as in this case the contribution due to the increase of interfacial area becomes important. After the critical point the contribution of entrained bubbles interfacial area increasingly contributes to the observed k_La increase.

In Fig. 6a and 6b experimental mass transfer coefficients obtained in the presence of the internal draft tube (left, H=2T; right, H=3T) are compared with the relevant results obtained in the configurations without internal draft tube. As it is possible to see, at the same specific power input the mass transfer coefficients obtained without draft tube are higher than those obtained in the configurations with the internal draft tube. This can be easily explained by the fact that the presence of the internal draft tube adds a friction solid surface inside the reactor which increases power dissipation requirements to obtain the same mass transfer performance. Also comparison of results between H=2T and H=3T cases shows that brim vicinity to liquid level at rest does not seem to entail particular performance improvements.

It is worth noting that, as already pointed out, in order to avoid gas dispersion inside the reactor, so preserving cells from bubble burst damage, an operating agitation speed smaller than the critical one (N_{crit}) should be used. In both the configurations with the internal draft tube, this implies a

maximum k_La of the order of $5{,}01*10^{-3}$ s^{-1} for the H=2T configuration and of $5{,}95*10^{-3}$ s^{-1} for the H=3T configuration as reported in Table 1 or by black symbols in Fig. 6a and 6b. These values are much higher than the relevant values obtained in the no-draft tube configuration (about $1{,}7*10^{-3}$ s^{-1}) and also higher than the typical maximum (critical) k_La values observed in unbaffled tanks with aspect ratio of 1 and stirred with a Rushton turbine (k_La_{crit} of about $1.3*10^{-3}$) or with an A310 impeller (k_La_{crit} of about $3.5*10^{-3}$ s^{-1}, [14]). It can be concluded that the addition of an internal draft tube in the bioreactor investigated, allows to significantly increase the mass transfer performance in sub-critical conditions (though in conjunction with a larger power demand) and therefore is particularly promising as a bioreactor for animal cells cultivation, if greater concentrations of cultured cells are sought (larger oxygen uptake rates requested) and bubble burst damage is to be avoided.

4. CONCLUSIONS

Oxygen transfer performance of large aspect ratio stirred vessels, either equipped or not with an internal draft tube, has been presented in view of their use as biochemical reactors for shear sensitive cells growth. As a matter of fact, oxygen mass transfer can conveniently occur through the quite wide free vortex surface which forms when agitation is large enough, yet still insufficient to inject bubbles in the liquid, so bubble subsequent bursting and related cell damage is avoided.

On the basis of present experimental results, one can predict that, for instance, this kind of bioreactor can provide sufficient oxygen mass transfer for animal cell growth at currently adopted cell concentrations in culture broths. The addition of an internal draft tube allows to further improve the maximum Oxygen transfer rate (OTR) achievable still in the absence of gas dispersion (*sub-critical conditions*), and may therefore become a particularly interesting configuration for shear

sensitive cells cultivation, should cell concentrations larger than those currently employed in the biotech industry be sought.

NOMENCLATURE

a: gas-liquid interfacial area per unit volume of dispersion [m^{-1}]

C: impeller clearance [m]

C_L^0: initial oxygen concentration in the liquid phase [kmol m^{-3}]

C_L: instantaneous oxygen concentration in the liquid phase [kmol m^{-3}]

C_L^*: equilibrium oxygen concentration [kmol m^{-3}]

D impeller diameter [m]

Fr Foude number $Fr = \frac{N^2 D}{g}$ [-]

H liquid height [m]

k_L: oxygen mass transfer coefficient [m s^{-1}]

$k_L a$ volumetric mass transfer coefficient [s^{-1}]

N rotational speed [rpm]

N_{crit} critical rotational speed [rpm]

N_p Power number [-]

OTR Oxygen Transfer Rate

P Power input [W]

P/V Specific power input [W m^{-3}];

Re Reynolds number $\mathrm{Re} = \frac{\rho_L N D^2}{\mu}$ [-]

SDPM simplified dynamic pressure method

t time [s]

t_0 initial time

T tank diameter [m]

V Tank volume [m^3]

Greek letters

ΔH Vortex depth [m]

μ liquid viscosity [Pa*s]

ρ_L liquid density [kg/m^3]

REFERENCES

[1] Busciglio A., Grisafi F., Scargiali F., Brucato A., 2014, Mixing dynamics in uncovered unbaffled stirred tanks, *Chemical Engineering Journal*, 254, 210-219.

[2] Scargiali F., Busciglio A., Grisafi F., Tamburini A., Micale G., Brucato A., Power consumption in uncovered-unbaffled stirred tanks: influence of viscosity and flow regime, *Industrial & Engineering Chemistry Research*, 52, Issue 42, (2013) 14998-15005

[3] B. Mazzarotta, Communication phenomena in stirred sugar suspensions, AIChE Symp. Ser. 89 (1993) 112–117.

[4] Assirelli, M., Bujalski,W., Eaglesham, A., Nienow, A.W., Macro- and micromixing studies in an unbaffled vessel agitated by a Rushton turbine. *Chem. Eng. Sci.*, 63 (2008) 35-46.

[5] Tamburini A., Brucato A., Busciglio A., Cipollina A., Grisafi F., Micale G.; Scargiali F., Vella G. , Solid−Liquid Suspensions in Top-Covered Unbaffled Vessels: Influence of Particle Size, Liquid Viscosity, Impeller Size, and Clearance. *Industrial & Engineering Chemistry Research*, 53, (2014) 9587-9599.

[6] Conway, K., Kyle, A., Rielly, C.D., Gas–liquid–solid operation of a vortex-ingesting stirred tank reactor, Chem. Eng. Res. Des., 80, (Part A), 2002, 839–845.

[7] Scargiali F., Russo R., Grisafi F. Brucato A, Mass Transfer and Hydrodinamic Characteristics of a High Aspect Ratio Self-Ingesting Reactor for Gas-Liquid Operations, Chemical Engineering Science, 62, N° 5 (2007) 1376 – 1387

[8] Scargiali F., Busciglio A., Grisafi F., Brucato A., Gas-liquid-solid Operation of a High Aspect Ratio Self-ingesting Reactor, *Int. J. Chem. React. Eng*., 10, Issue 1(2012) A-27, DOI: 10.1515/1542-6580.3011

[9] Grisafi F., Brucato A., Rizzuti L., 1994, Solid-liquid mass transfer coefficient in mixing tanks: influence of side wall roughness, IChemE Symp. Series, 136, 571-578.

[10] Brucato A., A. Cipollina, F. Grisafi, F. Scargiali, A. Tamburini, 2010, Particle suspension in top-covered unbaffled tanks, *Chemical Engineering Science*, 65, 3001-3008.

[11] Chisti Y., 2000, Animal-cell damage in sparged bioreactors, Tibtech Reviewes, 18, 420-432.

[12] Nienow A.W., Langheinrich C., Stevenson N.C., Emery A.N., Clayton T.M., Slater N.K.H., Homogenisation and oxygen transfer rates in large agitated and sparged animal cell bioreactors: Some applications for growth and production, *Cytotecnology*, (1996) 22, 87-94.

[13] Busciglio A., Caputo G., Scargiali F., Free-surface shape in unbaffled stirred vessels: experimental study via digital image analysis, *Chemical Engineering Science*, 104 (2013) 868-880

[14] Scargiali F., Busciglio A., Grisafi F., Brucato A. , Mass transfer and hydrodynamic characteristics of unbaffled stirred bio-reactors: influence of impeller design, *Biochemical Engineering Journal*, 82 (2014) 41- 47

[15] Scargiali F., Busciglio A., Grisafi F., Brucato A., Simplified Dynamic Pressure Method for k_La measurement in aerated bioreactors, *Biochemical Engineering Journal*, (2010) 49, 165-172

[16] Nagata, S., 1975. Mixing: Principles and Applications. Wiley, New York.

[17] Harnby N., Edward M.F. and Nienow A.W. 1985, (Eds.) Mixing in the Process Industries, Butterworth

[18] Paul E.L., Atiamo Obeng V.A., Kresta S.M., 2004, "Handbook of Industrial Mixing", Wiley and Sons

[19] Fenge C., Klein C., Heuer C., Siegel U., Fraune E., Agitatio, aeration, and perfusion modules for cell culture bioreactors, . , 11 (1993) 233-244.

Figure Captions

Fig. 1: Schematic diagram of the experimental apparatus*: a - left*) configuration without draft tube; *b - center)* configuration with internal draft tube and H=3T*; c - right)* configuration with internal draft tube and H=2T

Fig. 2: Experimental specific power input P/V [W m^{-3}] versus rotational speed N [rpm] for the five reactor configurations investigated. The straight line indicate a power low of 3. Black symbols indicate transition to aerated regime.

Fig. 3: Experimental Power Number N_p versus Reynolds number Re for the five reactor configurations investigated. Black symbols indicate transition to aerated regime.

Fig. 4 Experimental mass transfer coefficient *vs* rotational speed for the three reactor configurations investigated. Solid symbols mark the critical rotational speed (N_{crit}) and relevant mass transfer coefficients. Dashed horizontal line represents minimum k_La requirements for animal cell culture, according to Fenge *et al*.[19].

Fig. 5: Experimental mass transfer coefficient *vs* specific power dissipation for the configuration without internal draft tube and three different liquid volumes investigated. Solid symbols mark the critical specific power input (P/V_{crit}) and relevant mass transfer coefficients. Dashed horizontal line represents minimum k_La requirements for animal cell culture, according to Fenge *et al*.[19].

Fig. 6: Comparison between experimental mass transfer coefficient obtained in the configurations with and without the internal draft tube for H=2T (a) and H=3T (b). Solid symbols mark the critical specific power input (P/V_{crit}) and relevant mass transfer coefficients. Dashed horizontal lines represents the k_La range requirements for animal cell culture according to Fenge *et al*.[19].

Tab. 1: Bioreactor configurations investigated and relevant critical rotational speeds (N_{crit}), Reynolds number (Re_{crit}), specific power inputs (P/V_{crit}) and mass transfer coefficients k_La_{crit}.

Liquid level	Draft tube	N_{crit} [rpm]	Re_{crit} [-]	P/V_{crit} [W/m^3]	k_La_{crit} [s^{-1}]
H=T	No	550	82700	450	1,80*10^{-3}
H=2T	No	700	105300	649	1,68*10^{-3}
H=3T	No	850	128000	860	1,67*10^{-3}
H=2T	YES	815	122600	1390	5.01*10^{-3}
H=3T	YES	1050	158000	2100	5.95*10^{-3}

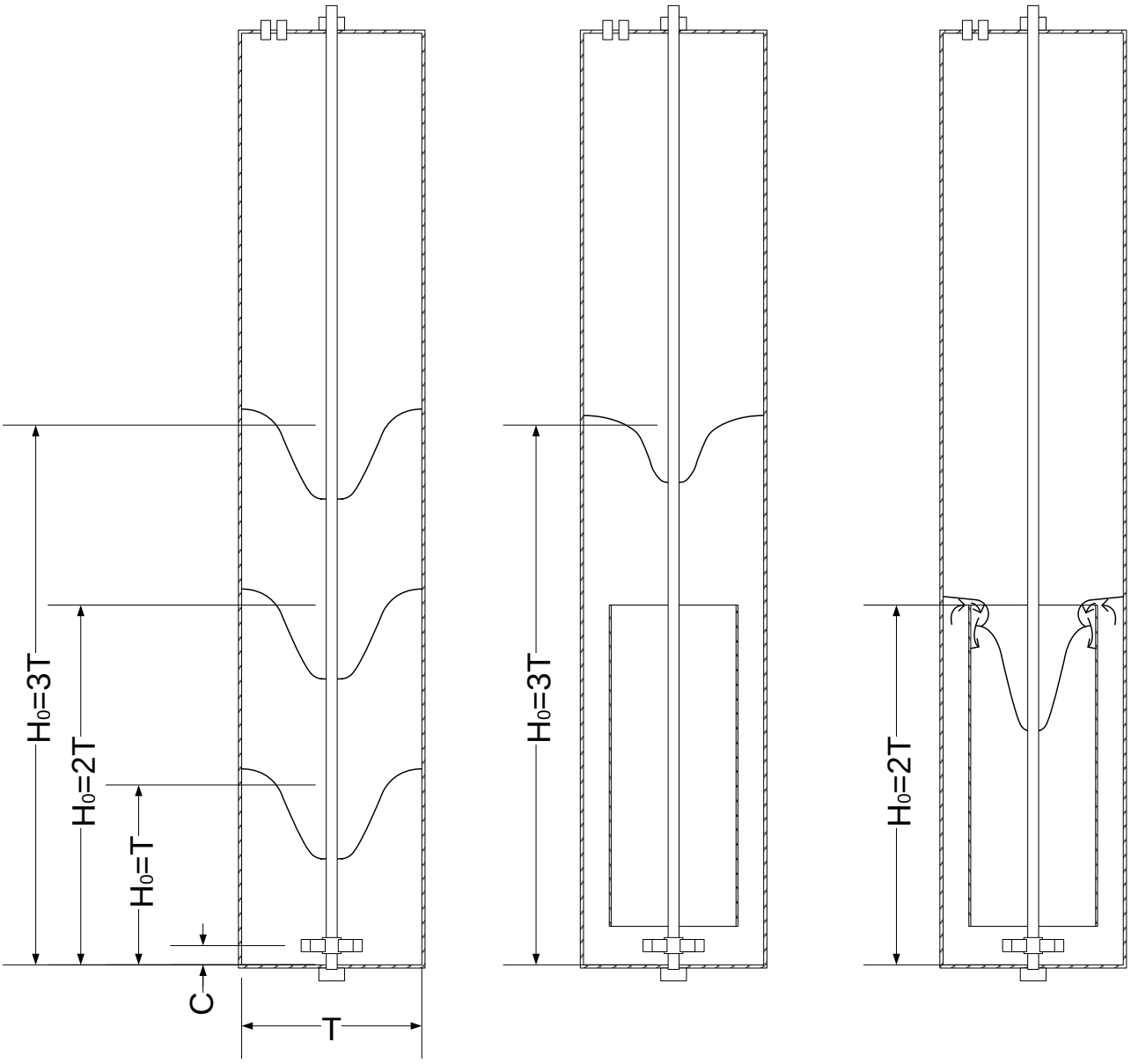

Fig. 1: Schematic diagram of the experimental apparatus: *a* - *left*) configuration without draft tube; *b* - *center*) configuration with internal draft tube and H=3T; *c* - *right*) configuration with internal draft tube and H=2T

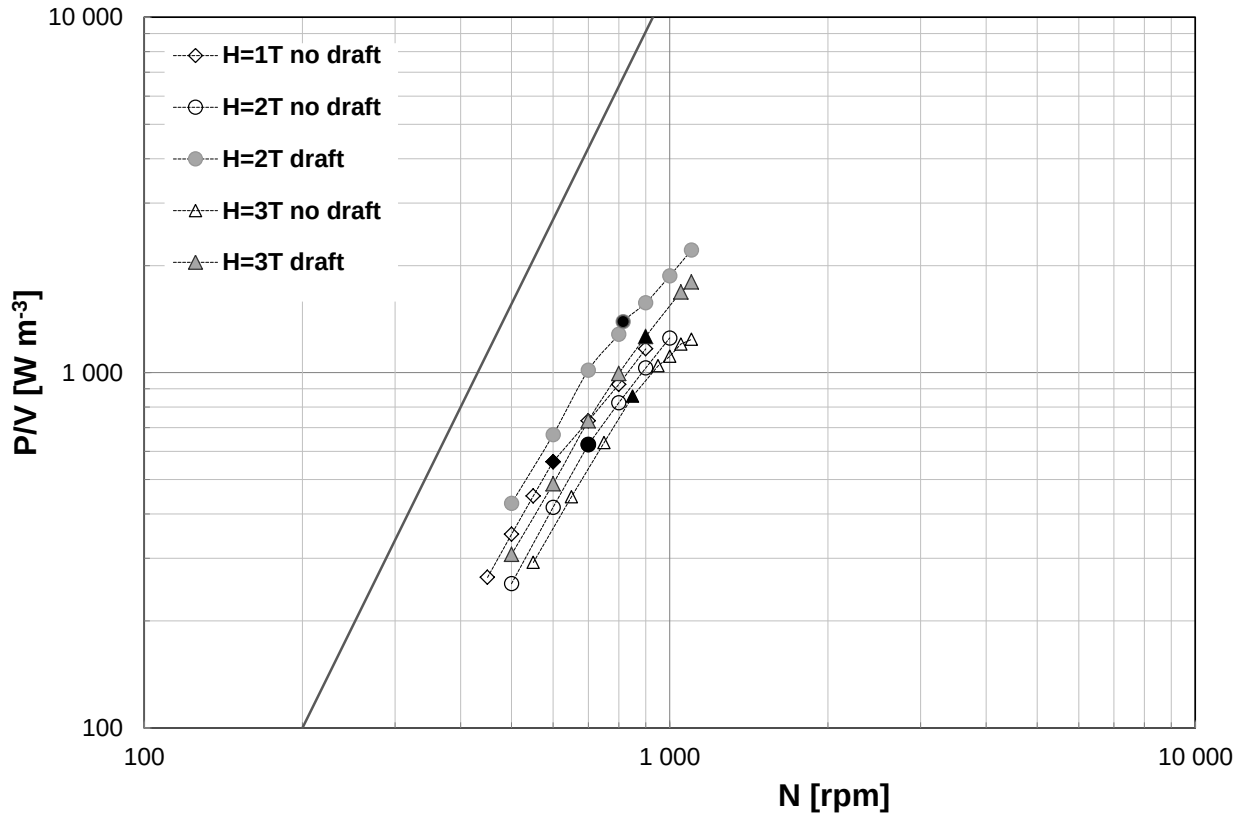

Fig. 2: Experimental specific power input P/V [W m^{-3}] versus rotational speed N [rpm] for the five reactor configurations investigated. The straight line indicate a power low of 3. Black symbols indicate transition to aerated regime.

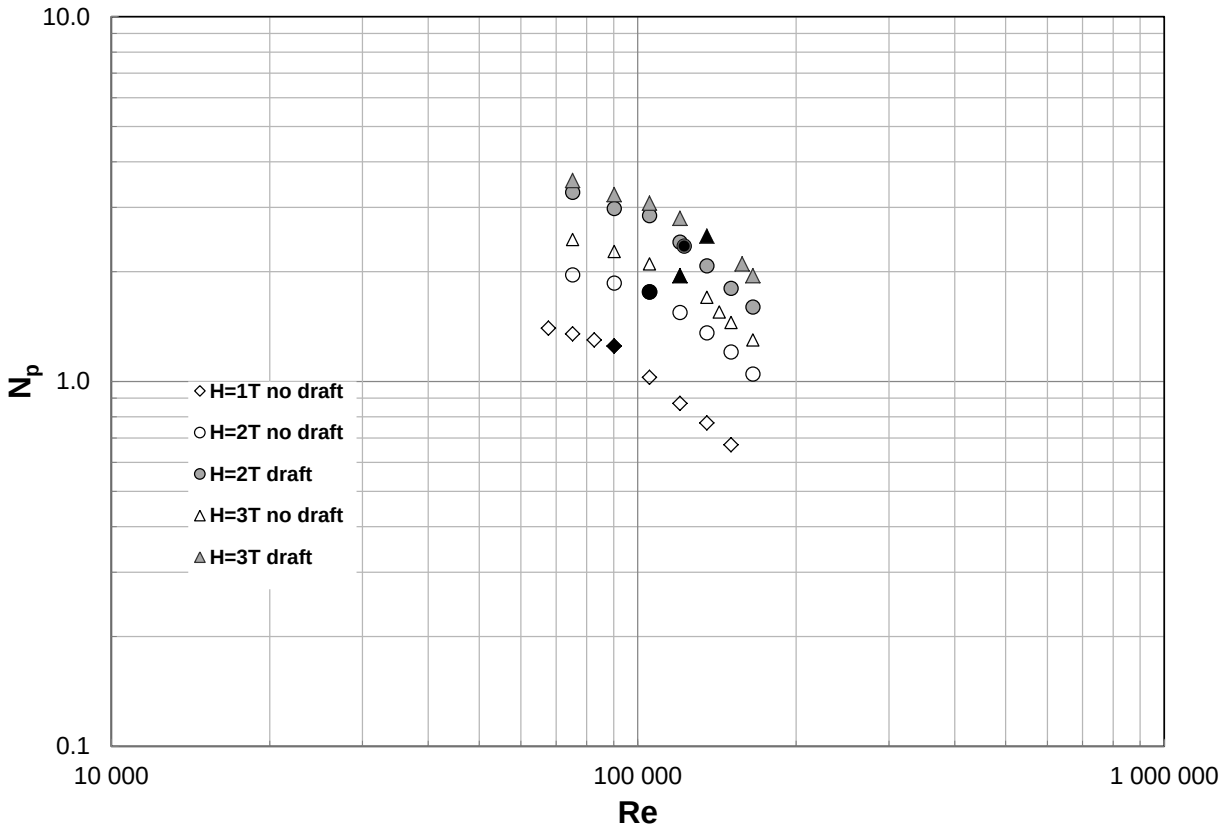

Fig. 3: Experimental Power Number N_p versus Reynolds number *Re* for the five reactor configurations investigated. Black symbols indicate transition to aerated regime.

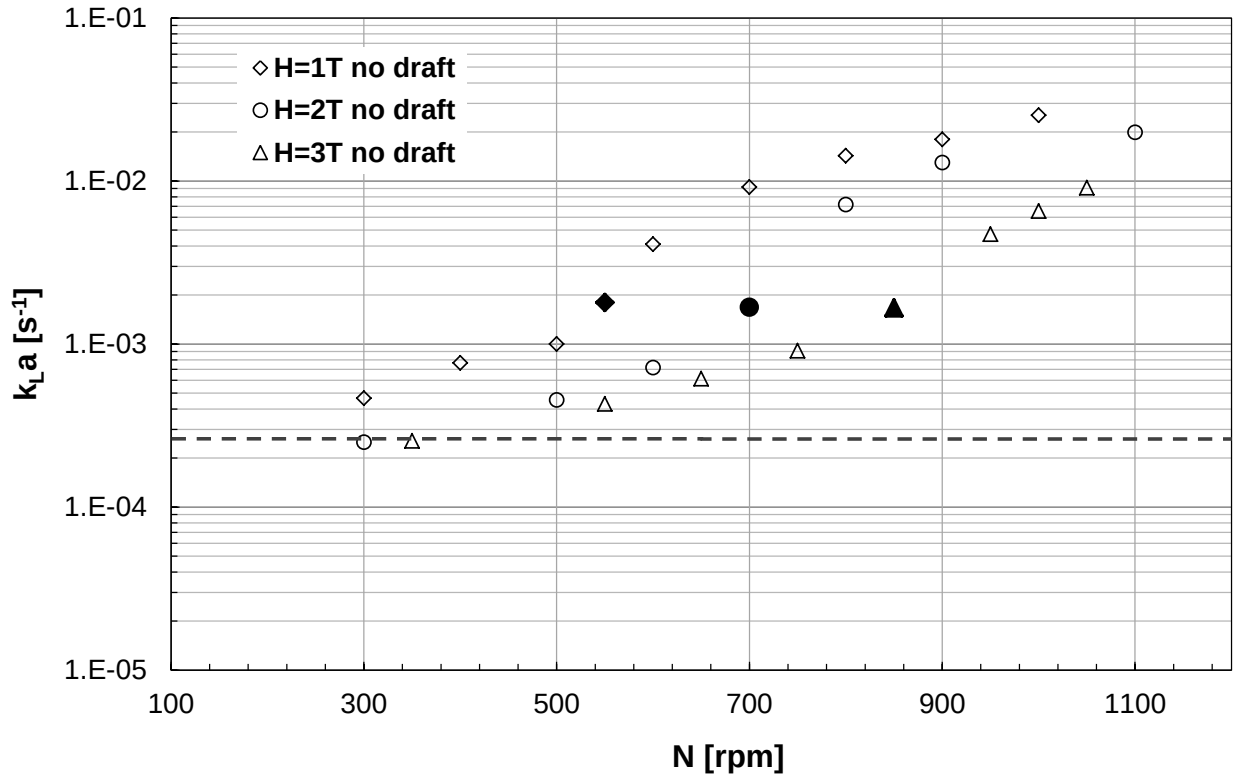

Fig.4: Experimental mass transfer coefficient *vs* rotational speed for the three reactor configurations investigated. Solid symbols mark the critical rotational speed (N_{crit}) and relevant mass transfer coefficients. Dashed horizontal line represents minimum k_La requirements for animal cell culture, according to Fenge *et al*.[19].

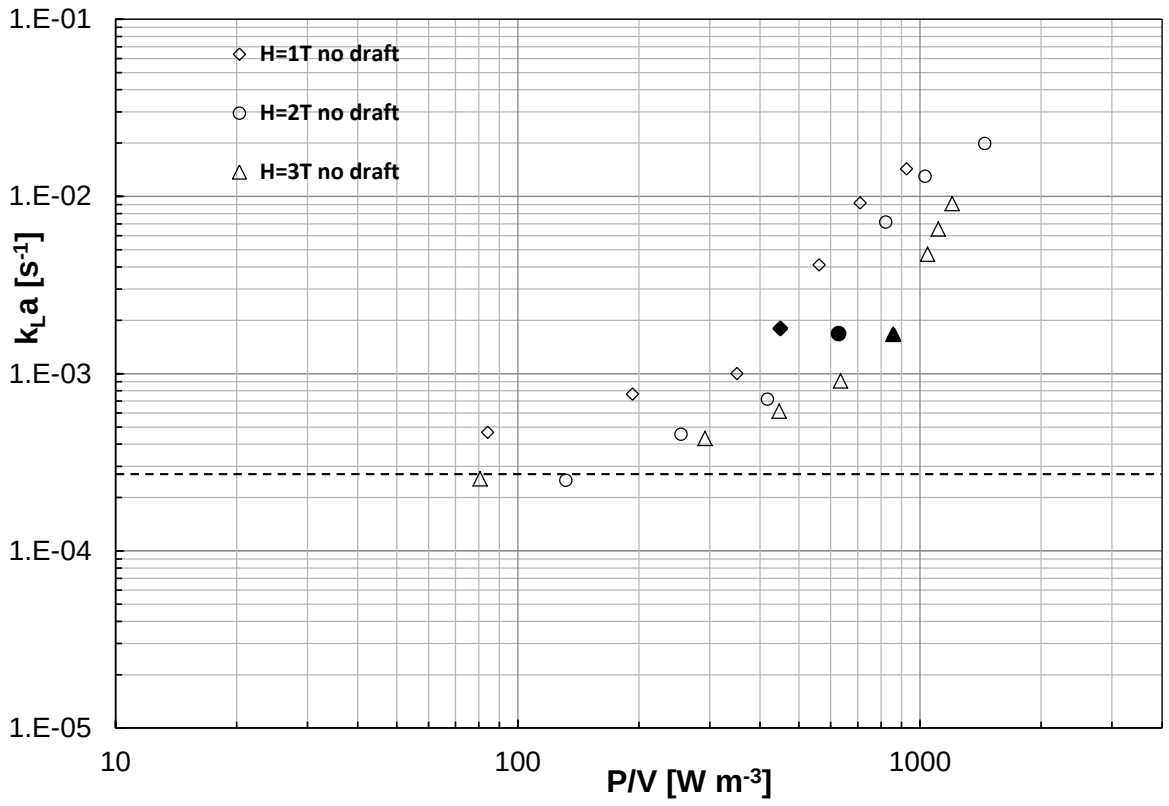

Fig. 5: Experimental mass transfer coefficient *vs* specific power dissipation for the configuration without internal draft tube and three different liquid volumes investigated. Solid symbols mark the critical specific power input (P/V_{crit}) and relevant mass transfer coefficients. Dashed horizontal line represents minimum k_La requirements for animal cell culture, according to Fenge *et al*.[19].

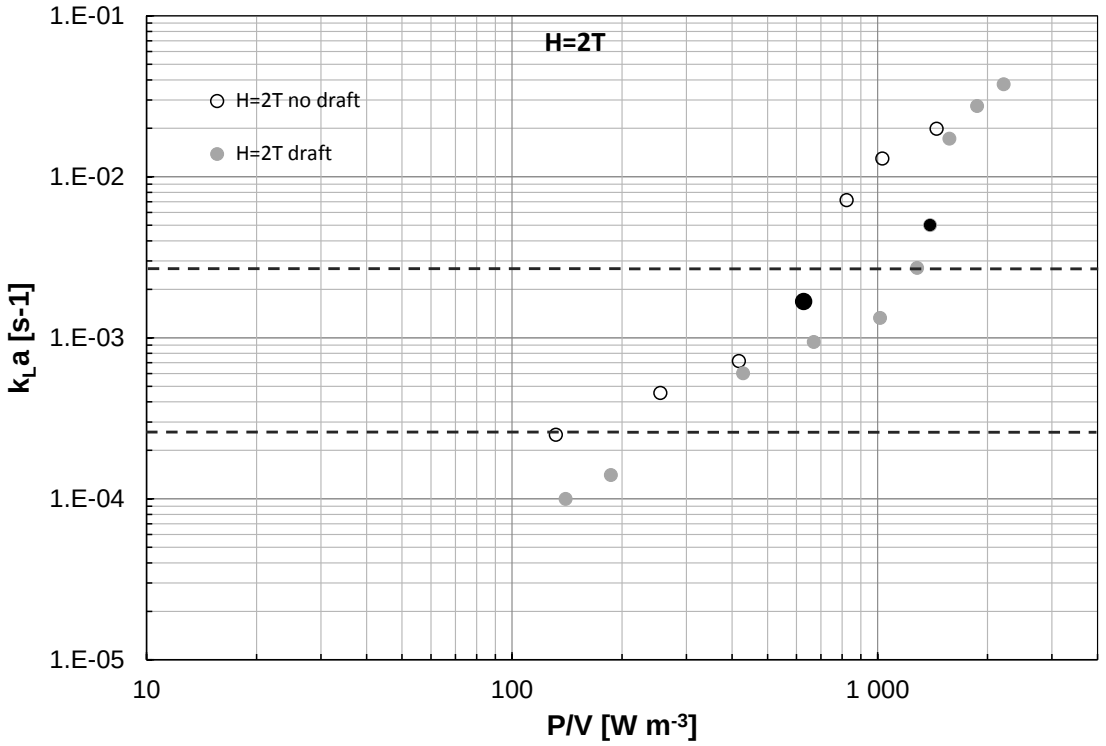

a)

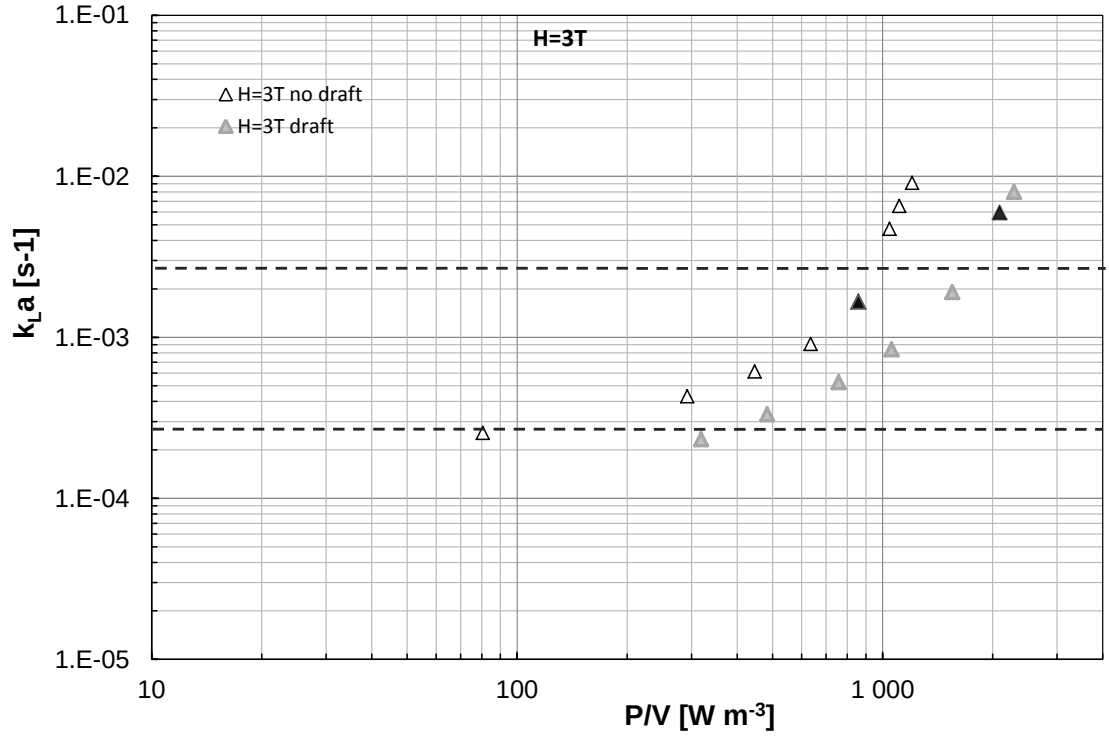

b)

Fig. 6: : Comparison between experimental mass transfer coefficient obtained in the configurations with and without the internal draft tube for H=2T (a) and H=3T (b). Solid symbols mark the critical specific power input (P/V_{crit}) and relevant mass transfer coefficients. Dashed horizontal lines represents the k_La range requirements for animal cell culture according to Fenge *et al*.[19].